Journal of Sound and Vibration (1996) **198**(3), 267–277

THE SIGNIFICANCE OF HIGHER MODES FOR EVOLUTION OF CHAOS IN STRUCTURAL MECHANICS SYSTEMS

R. I. K. Moorthy and A. Kakodkar

Reactor Design and Development Group, Bhabha Atomic Research Centre, Bombay 400 085, *India*

AND

H. R. Srirangarajan

Department of Mechanical Engineering, Indian Institute of Technology, Powai, Bombay 400 076, *India*

(*Received* 9 *November* 1994, *and in final form* 22 *April* 1996)

Even though chaotic vibrations have been observed in many structural mechanics systems, their analysis has almost always been limited to single-degree-of-freedom (SDOF) approximations. A typical example is the magnetoelastic beam studied by Moon and Holmes [1], which is reported to be the first experimental evidence of chaotic vibrations in structural mechanics. However, the authors have not come across any detailed structural analysis of the system. The present paper reports a structural dynamic analysis of the problem through a finite element formulation and the integration of the resulting equations of motion by a variable time stepping Newmark method (trapezoidal rule). The solution scheme has built-in algorithms for equilibrium iteration of the non-linear forces and check of the temporal solution trajectory. It is shown that the direct integration and mode superposition schemes are equally applicable for problems with chaotic response. The authors have the following conclusions: (1) the SDOF approximation with a high accuracy integration scheme may not reveal the regime of chaos even coarsely; (2) the manifestation of chaos is significantly influenced by the higher modes; (3) a spatially discrete model which represents the beam accurately could reveal regimes of chaos reasonably well even with second order schemes such as the trapezoidal rule, but it is essential for the model to be fine enough to represent the motion in higher modes accurately; (4) computationally efficient methods such as the mode superposition method, with an adequate number of modes included, could give accurate solutions to vibration problems involving chaos.

1. INTRODUCTION

There are many structural mechanics systems that are known to respond chaotically [2]. The analytical simulation of these systems has almost always been restricted to single-degree-of-freedom (SDOF) approximations. If the physical properties of a system are such that its motion could be described by a single co-ordinate and no other motion is possible, then it actually is a SDOF system and the solution of the equation provides the exact dynamic response. On the other hand, if the structure has more than one possible mode of displacement and it is reduced mathematically to a SDOF approximation by assuming its deformed shape, the solution of the equation of motion is only a coarse approximation of the true dynamic behavior. The solution of such a coarse model by using higher accuracy integration schemes such as the fourth or higher order Runge–Kutta

0022–460X/96/480267 + 11 $25.00/0

scheme may not bear much resemblance to the actual response unless the system is constrained to move in the assumed shape.

In general, even for linear problems, the dynamic response of the structure cannot be described adequately by a SDOF model; it usually includes a response in more than one DOF. In this paper the solution is reported of multi-degree-of-freedom (MDOF) model of a chaotic vibration problem and the number of degrees of freedom/modes required to be included to obtain results comparable with the experimental results available in the literature is investigated. The problem chosen for the study is the magnetoelastic beam studied by Moon and Holmes [1]. This problem has been chosen as this was the first experimental evidence of chaotic vibration in structural mechanics and a large quantity of experimental results are available for comparing the analytical results being generated. Also, the authors have not come across any analytical simulation of this problem beyond the SDOF, even though the experimental results have been available for the past 15 years. Although Tang and Dowell [3] have investigated the effect of higher modes in another similar problem, they conjectured that higher modes are significant only in their case and not in the case of the problem studied by Moon and Holmes. In fact, in this paper the validity of this conjecture is also examined.

2. EXPERIMENTAL SET-UP USED BY MOON AND HOLMES [1]

The experimental apparatus studied by Moon and Holmes (see Figure 1) consisted of a cantilevered beam, permanent magnets, a vibration shaker and strain gauge recording devices. The beam was made from a steel rule 0·23 mm (0·009 in) thick, 9·5 mm (3/8 in) wide and 18·8 cm (7·4 in) long. The beam was clamped vertically at one end and suspended at the other end between two rare earth magnets. The 2·54 cm (1·0 in) diameter magnets were secured to a steel base. This base and the beam clamp were attached to a wooden plate, which was driven by an electromagnetic shaker.

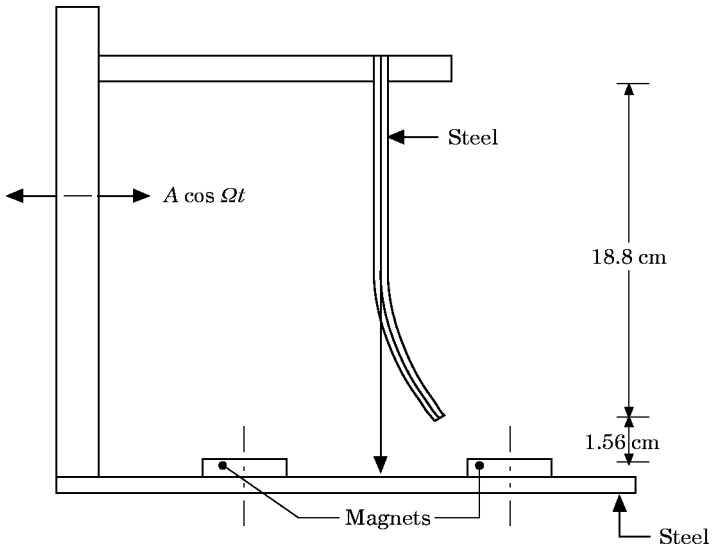

Figure 1. The experimental apparatus, showing the ferroelastic beam and permanent magnets.

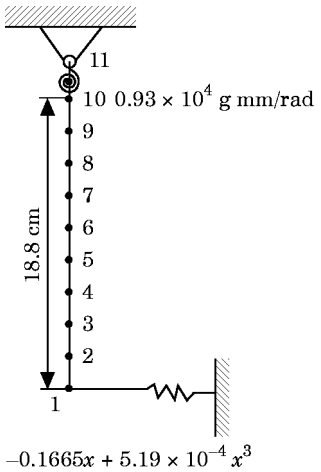

Figure 2. The finite element model of the magnetoelastic beam.

3. FINITE ELEMENT MODEL

The equation of equilibrium for a system assembled by a set of finite elements can be written as [4–7]

$$[K]\{y\}_{t+\Delta t} + [C]\{\dot{y}\}_{t+\Delta t} + [M]\{\ddot{y}\}_{t+\Delta t} = \{P\}_{t+\Delta t}, \tag{1}$$

Where $[K]$ is the stiffness matrix of the assembly, $[C]$ is the damping matrix, $[M]$ is the mass matrix, $\{P\}_{t+\Delta t}$ is the external load vector at the time $t + \Delta t$, and $\{y\}_{t+\Delta t}$, $\{\dot{y}\}_{t+\Delta t}$ and $\{\ddot{y}\}_{t+\Delta t}$ are the displacement, velocity and acceleration vectors at time $t + \Delta t$. The system matrices $[K]$, $[M]$ and $[C]$ can be obtained as follows.

3.1. STIFFNESS MATRIX $[K]$

The formation of the stiffness matrix for a straight, uniform beam element has been discussed in detail by many authors [4–7]. For the beam studied by Moon and Holmes [1], no effect of transverse shear deformation or axial load need be considered. (The effect due to magnetic forces is discussed separately.)

For a uniform cantilever of the geometry used in reference [1], the theoretical natural frequencies can be calculated from the closed form solution [8] as 5·34 Hz, 33·38 Hz and 93·6 Hz. However, the first three natural frequencies without the magnets have been reported by Moon and Holmes [1] as 4·6 Hz, 26·6 Hz and 73·6 Hz. Such a reduction in the actual natural frequencies is not uncommon in engineering structures. This is due to the small rotations that are rendered possible at the clamped end of the assembly. This could be modelled analytically by incorporating a rotational spring of appropriate stiffness at the support location [9–11]. To determine this rotational spring stiffness, the cantilever was modelled as shown in Figure 2 and solved for the eigenvalues. A rotational spring stiffness of 0·93 kg cm/rad realizes the natural frequencies of 4·4 Hz, 28·6 Hz and 81·6 Hz; that is, the fundamental frequency within 4% and the lowest three frequencies within 10%. By a combination of translation and rotational springs, it would be possible to bring the analytical frequencies closer. However, for the present study of the relative significance of the higher modes, the model shown in Figure 2 represents the experimental beam adequately.

3.2. MASS MATRIX [M]

In the finite element formulation of the mass matrix, there are two approaches: the lumped mass and the consistent mass. The most common approach is the lumped mass, wherein the masses (translational and rotational) are assumed to be lumped at the nodes of the elements, thus giving a diagonal matrix. In the consistent mass concept, the inertia force at each node is consistent with the static deflection curve, thus giving rise to off-diagonal terms and consequent higher computational effort. However, for the same element discretization, dynamic analysis using a consistent mass matrix gives results which approximate closer to the exact solution than those of the lumped mass method. The applicability of both approaches has been studied for the present problem and is reported in later sections.

3.3. DAMPING MATRIX [C]

The various numerical treatments to account for damping have been reviewed by Belytschko and Mindle [12]. A Rayleigh proportional damping expressed as $[C] = \beta[M] + \gamma[K]$ is used for the analysis. The constants β and γ can be determined if the damping is known at two frequencies. Moon and Holmes [1] have reported a modal damping of 0·0036 for the first mode. This has been used to generate a stiffness proportional damping: that is, $\beta = 0$ and $\gamma = 5{\cdot}64743\text{D}-05$ have been used for the analysis.

To generate the Poincaré map, constrained layer damping has been introduced by Moon and Holmes in the experiment. This is considered later in Section 8.

4. SIMULATION OF THE MAGNETIC FORCES

Moon and Holmes [1] have shown that the magnetic forces in the configuration used for the experiment could be represented by a small constant axial force and a bending load, F_{NL}, given by $F_{NL} = Ax + Bx^3$. The following data is also available from the experimental set-up.

(1) In the presence of the magnets, the stable static equilibrium position is obtained at $x = \pm 16{\cdot}8$ mm: that is,

$$(K_{beam} + A)x + Bx^3 = 0 \qquad \text{at } x = \pm 16{\cdot}8 \tag{2}$$

(2) The lowest natural frequency for small amplitudes of vibration about this static equilibrium is 9·3 Hz. To realize this, the stiffness of a linear spring required to be incorporated at the tip has been calculated by the FEM code SAP-IV [13]. This is obtained as 0·273 g/mm. This means that the slope of the non-linear magnetic force around $x = 16{\cdot}8$ will be equal to 0·273 g/mm: that is

$$A + 3{\cdot}0Bx^2 = 0{\cdot}273 \qquad \text{at } x = \pm 16{\cdot}8 \tag{3}$$

From equations (2) and (3), A and B have been calculated as $A = -0{\cdot}1665$ and $B = 5{\cdot}19\text{E}-04$.

In these calculations, the tension due to the magnetic forces is assumed to be negligible and the change in the natural frequency is thus entirely due to the bending stiffness. This had to be done due to the unavailability of information necessary to separate the individual contributions. The probable effect of this is discussed further in Section 7.

5. SOLUTION SCHEME

The equation of motion [1] can now be written as

$$[M]\{\ddot{y}\}_{t+\Delta t} + \beta[M]\{\dot{y}\}_{t+\Delta t} + \gamma[K]\{\dot{y}\}_{t+\Delta t} + [K]\{y\}_{t+\Delta t} = P_{t+\Delta t} - F_{NL_{t+\Delta t}}. \tag{4}$$

Since the non-linearity is confined to the tip, putting the magnetic forces on the right side of equation (4) as an equivalent load avoids reformation of the stiffness matrix and its solution at each time step.

To obtain the solution of equation (4) a numerical integration technique has been used. The step-by-step integration method can be applied either to the coupled equations of motion as in equation (4) or to the uncoupled equations of motion after modal decomposition. For the present study, the mode superposition method, in addition to a considerable saving of computational effort, gives the number of modes contributing significantly to the chaotic response. In this paper, both the direct integration and mode superposition results are reported.

Of the many step-by-step integration procedures available, the fourth order Runge–Kutta scheme seems to be the preferred algorithm for chaos in lower order systems. It has an accuracy of the order of $(\Delta t)^4$, but requires four equation solutions per time step.

The finite element model of structures produces "stiff" equations: i.e., they characterize structures the highest natural frequency of which is very much greater than the lowest ($\omega_{max} > > \omega_{min}$). Even to solve linear problems by the Runge–Kutta method, such stiff equations need very small time steps and so the method is not favored for FEM applications. For non-linear problems modelled by FEM, the Runge–Kutta method would need time step that is much too small to undertake any long duration solution, which is essential to confirm chaos. In the assessment of the authors [14], the Newmark method (trapezoidal rule), with checks to ensure accuracy of the solution trajectory, is computationally efficient and accurate and is therefore used here. The integration scheme is briefly explained below.

5.1. INTEGRATION SCHEME

The Newmark method [4, 5] with operator constants of $\delta = 0{\cdot}5$ and $\alpha = 0{\cdot}25$ has been used for the integration, for the following reasons: (a) it offers unconditional stability when applied to linear problems; (b) there is no amplitude error, and the smallest period error; (c) there is only one set of implicit equations to be solved per time step; (d) it offers second order accuracy; and (e) it is self-starting.

The present problem of the cantilever represented by equation (4) can be shown to be [14, 15] $\bar{K}y_{t+\Delta t} = \bar{P}_{t+\Delta t} - \mathrm{F_{NL}}$, where

$$\bar{K} = K\left[\frac{1+\gamma\delta}{\alpha\Delta t}\right] + M\left[\frac{1+\beta\delta\Delta t}{\alpha\Delta t^2}\right],$$

$$\bar{P}_{t+\Delta t} = P_{t+\Delta t} + M\left[\left\{\frac{1}{\alpha\Delta t^2} + \frac{\beta\delta}{\alpha\Delta t}\right\}y_t + \left\{\frac{1}{\alpha\Delta t} - \beta\left(1-\frac{\delta}{\alpha}\right)\right\}\dot{y}_t + \left\{\frac{(0{\cdot}5-\alpha)}{\alpha} - \frac{\beta\,\Delta t}{2}\left(2-\frac{\delta}{\alpha}\right)\right\}\ddot{y}_t\right] + K\left[\frac{\gamma\,\delta}{\alpha\,\Delta t}y_t + \left(\frac{\delta}{\alpha}-1\right)\gamma\dot{y}_t + \frac{\gamma\,\Delta t}{2}\left(\frac{\delta}{\alpha}-2\right)\ddot{y}_t\right],$$

$$F_{NL_{t+\Delta t}} = Ay_{t+\Delta t} + \mathrm{By^3}_{t+\Delta t}.$$

The solution at time $t + \Delta t$ is iterative in nature, as F_{NL} is dependent on the displacement being solved. The initial trial value of F_{NL} for the iteration is obtained by extrapolation of the F_{NL} values of the previous solution steps.

The convergence of the iteration is measured by the ratio of the difference between the current and the previous iterates of F_{NL} and the current value of F_{NL}. Convergence of the order of 1·0E−06 is normally achieved within a few iterations. If not, the time step is reduced, which hastens the convergence [14, 15].

5.2. TIME-STEP ERROR CONTROL

In addition to the control on step length to ensure the convergence of F_{NL}, the error associated with the time-stepping solution needs to be contained. In respect to the application of the solution scheme for problems with chaotic response, it is essential to follow the solution trajectory closely. The present integration scheme is based on the assumption of linear variation of the acceleration over a time step, and so it is possible to interpolate the solution at any intermediate point. Since the dynamic equilibrium needs to satisfied all along the solution trajectory, any "residue" obtained at any intermediate point is the error or the deviation from the actual solution trajectory. It has been found [14, 15] that a tolerance of 1% of the maximum force on the half-step residue gives accurate results.

6. ACCEPTABLE PARAMETERS FOR THE ANALYTICAL MODEL

To arrive at an acceptable analytical model, the following two parameters are studied: (1) the number of degrees of freedom/number of elements; (2) lumped mass versus consistent mass modelling.

In fact, the number of degrees of freedom also gives an indication of the number of significant modes in which the beam is responding, and it is necessary to include it to obtain results comparable to the experimental results. To obtain the above parameters, the problem was solved repeatedly for an excitation frequency of 8·3 Hz, with the excitation amplitude increasing, starting from a small value until chaos was observed. This excitation frequency has been chosen because it was at this frequency that Moon and Holmes found experimentally that the amplitude of excitation required to obtain chaos was least.

6.1. METHOD USED FOR IDENTIFICATION OF CHAOS

It was reported [1] that in the case of non-existence of chaos at any point in the forcing frequency–amplitude plane, the beam might exhibit chaos initially but settle into a periodic motion within one minute. Accordingly, the experimental values reported by Moon and Holmes [1] were those points at which the chaotic motion continued for more than one minute. Accordingly, the chaotic response is confirmed in the present analysis by examining the Poincaré plot of 999 points after the first 333 points which are discarded to eliminate the effect of transients. In other words, the solution has been carried out for 1332 load cycles. The strain and strain rate have been used for the Poincaré plot, both for the experimental results of Moon and Holmes [1] and the results reported here.

6.2. ACCEPTABLE VALUES OF PARAMETERS

In Figure 3 is shown the minimum excitation level for chaos as a function of the number of degrees of freedom of the model. The figure shows two curves: one for the lumped mass case and the other for the consistent mass case. The following can be observed from the figure.

(a) *Lumped mass modelling*. At least a 21-DOF model (ten-element discretization of the beam) is required to obtain chaos at an excitation value reported experimentally [1]. With coarser discretization, the excitation level required for chaos is higher, and going finer beyond ten elements does not significantly change the minimum excitation level required for chaos. This also gives an idea of the number of modes required to characterize the response adequately. Dobson [16] has expressed the view that only 40% of the modes corresponding to the translational degrees of freedom are realistic. This, in the present case, would mean that three to four modes are required to be included to obtain accurate response. However, a one-mode approximation would be grossly in error. The actual number required to be included is addressed in section 7.

(b) *Consistent mass modelling*. As is to be expected, consistent mass modelling approximates the exact results better than the lumped mass at a smaller number of degrees of freedom. Here again, as the discretization becomes finer, the results of both the lumped mass and consistent mass formulations give results comparable with each other, as well as with the experimental results; see Figure 3. This is in line with the observation [5] that consistent mass matrices are more accurate for flexural problems such as those of beams and shells, but negligibly so if the wavelength of the mode spans more than about four elements. It can be observed form Figure 3 that beyond ten elements (21 DOF) there is a negligible difference between the lumped mass and consistent mass results. The fact that a five-element (11-DOF) lumped mass model shows a large error, compared to the consistent mass as well as the experimental results, suggests that more than one mode is contributing to the chaotic response. Furthermore, upon noting that the results of the ten-element model obtained by both the lumped and consistent mass approaches are the same, and keeping in mind the mode shapes for higher modes of the cantilever, it can be estimated that about three modes could be contributing to the chaotic response. The actual number of modes contributing to the chaotic response could be found if modes superposition analysis is applicable to chaos, and this is considered in the next section.

7. APPLICABILITY OF MODE SUPERPOSITION METHOD AND NUMBER OF MODES CONTRIBUTING TO THE CHAOTIC RESPONSE

Instead of directly integrating the coupled equations of motion represented by the [K], [M] and [C] matrices, the uncoupled equations of motion corresponding to each of the modes could be solved and superposed to obtain the total response [4–6]. The computation

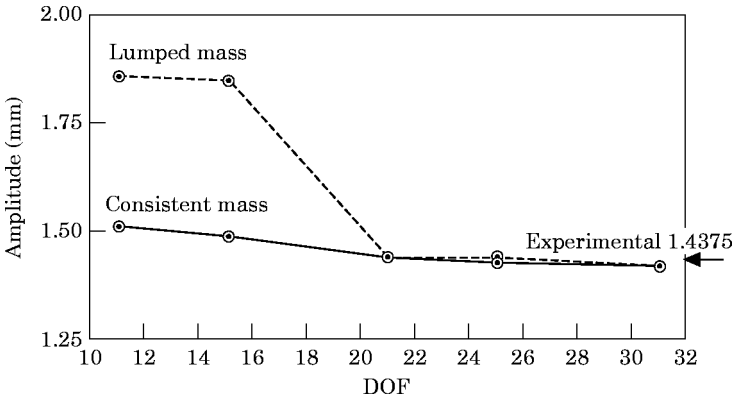

Figure 3. The number of DOFs required for chaos.

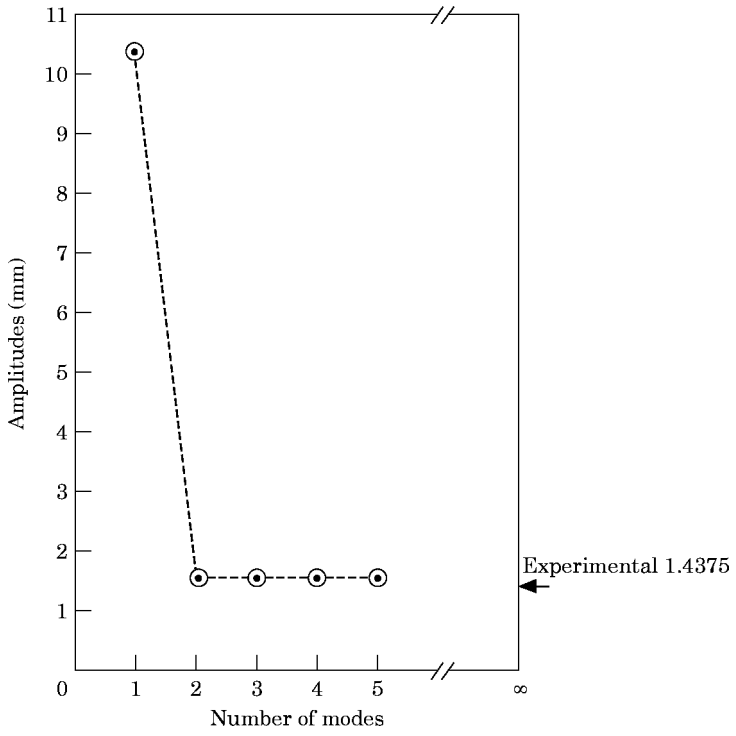

Figure 4. The number of modes required to simulate chaos.

expense of such a model is orders of magnitude lower and also the number of modes contributing significantly to the response could be exactly determined. Such a solution was carried out starting from eigenvalues and eigenvectors calculated for a finely discretized beam. The tip displacement at each time step due to each mode was superposed and the F_{NL} was computed iteratively until convergence of the F_{NL} to 1·0E−06 was obtained.

As in the direct integration method of solution, here again the Poincaré map of 999 load cycles after the first 333 load cycles was used to confirm chaos.

The minimum amplitude required at the frequency of 8·3 Hz was computed by progressively including higher modes. The results are shown in Figure 4; here the abscissa is the number of modes included in the analysis and the ordinate is the minimum excitation amplitude at which chaos is observed. It is clear that a one-mode approximation is grossly inadequate, as the amplitude required to obtain chaos is eight times the experimental value. A solution by a more accurate integration scheme such as the fourth order Runge–Kutta scheme does not make any significant improvement. It can also be seen that the inclusion of modes beyond the third has no influence on the excitation required for chaos, thus confirming that three modes contribute significantly to the chaotic response.

The computational advantage of the solution of modal equations can be appreciated from the fact that it takes less than 3% of the time required to solve a 21-DOF finite element model by direct integration.

8. INVESTIGATION OF THE REGIME OF CHAOS

The above analysis is of engineering significance only if the model is able to define the regime of chaos comparable to the experimental results. The regime of chaos obtained

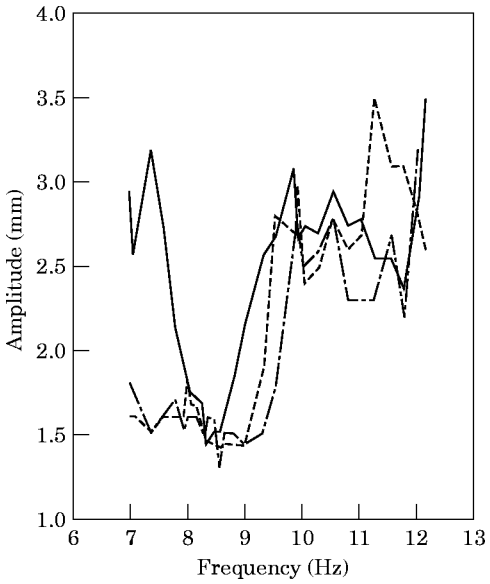

Figure 5. The chaotic regime in the forcing frequency – amplitude plane, ——, Experimental from reference [1]; – – –, analytical by mode superposition, three mode approximation; —·—·—, analytical by direct integration of the 21-DOF model.

analytically by direct integration as well as by mode superposition is shown in Figure 5. As earlier, the Poincaré map of 999 points after the first 333 load cycles has been used to confirm chaos. The figure also shows the experimental points as taken from reference [1].

The comparison of the analytical and experimental results shows that they match reasonably well. The slight inadequacies of the analytical model, such as the absense of tension and the assumption of stiffness proportional damping, could have contributed to the discrepancy between the analytical and experimental results. The information in reference [1] is not adequate to indentify the contributions from tension and lateral magnetic forces which, together, have increased the natural frequency of the beam to 9·3 Hz. Nevertheless the results can be considered to be highly satisfactory, as a better comparison may not easily be obtained for this structural dynamic problem.

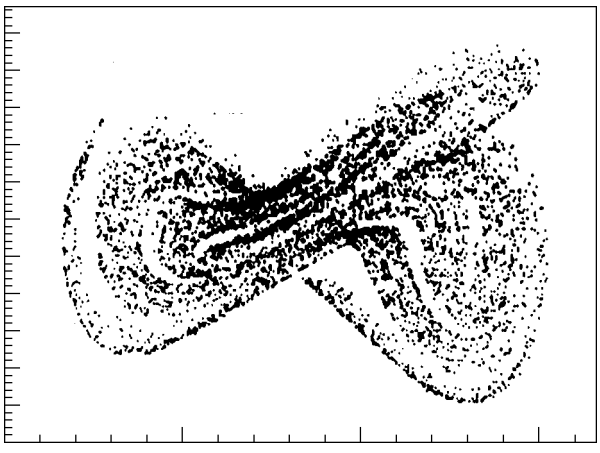

Figure 6. The Poincaré map of the damped magnetoelastic beam; present analysis.

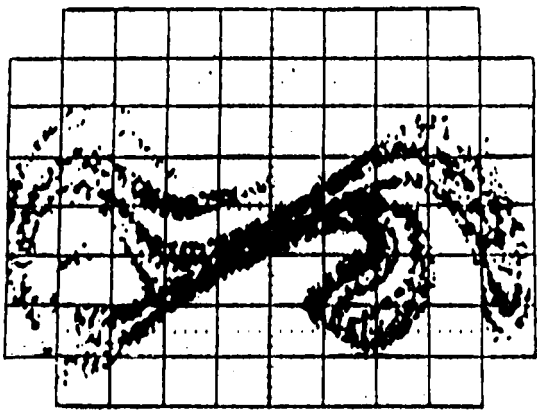

Figure 7. As Figure 6, but experimental [1].

9. POINCARÉ MAP OF THE DAMPED MAGNETOELASTIC BEAM

In undamped or lightly damped systems, the Poincaré maps of chaotic motions appear as a cloud of unorganized points in the phase plane. Therefore, in order to bring out the strange attractor features clearly in the experiment, Moon and Holmes added constrained layer damping to the beam. This was done by putting double sided sticky cellophane tape along the beam and attaching a thin steel layer of 0·05 mm thickness on top of this. This was done on both sides of the beam, and it increased the damping to 2·6% of the critical from 0·36% of the critical as seen on the bare beam.

It should be noted that by adding such steel strips, the mass of the system had been increased without increasing the stiffness. By adding the mass of 0·1 mm thick steel (0·05 on either side) and using the experimentally obtained damping, again as stiffness proportional damping, the Poincaré map has been generated analytically. This is shown in Figure 6. For comparison, the experimental Poincaré map from reference [1] is shown in Figure 7. Apparantly, similar features can be noted in the two figures.

10. CONCLUSIONS

Although chaotic vibrations have been observed for a long time, an analytical simulation suitable for any engineering application has been lacking. Almost always, a single-degree-of-freedom model has been used in conjunction with a higher order integration scheme. Such an analysis could, at best, bring out qualitatively that chaos could occur in the system. Such a coarse model cannot be used for identification of the regime of chaos or for studying the parameters influencing the chaotic response. To obtain the actual behavior of structures, it is essential to include all of the significant modes (and not just the lowest mode) which contribute to the total response. If the model is a good physical representation of the structure, lower order, stable integration schemes such as the trapezoidal rule would bring out the chaotic response accurately. Therefore, the important conclusion is that the trueness of the mathematical model of the structure is the most important aspect, and that the integration scheme is secondary to it. The fact that higher modes are significant is consistent with the observation of Tang and Dowell [3] for their experimental set-up. However, their conjecture that higher modes are not significant for the Moon and Holmes beam is not found to be true.

The beam studied here and that earlier in reference [15] are distributed systems having their stiffness and inertia distributed over the entire length. Mathematically, such systems are represented by partial differential equations. In solving the beam equations by the finite

element method, spatial discretization was carried out to obtain ordinary differential equations for each of the discrete spatial points. In addition, in any numerical integration scheme, the solution is temporally discrete. It can be seen that such a spatially and temporally discrete solution scheme captures the response accurately even when the response is chaotic. In fact, the motivation for this study has been the identification by Moon [17] of the need to confirm whether these can also give solutions where the response is known to be chaotic.

It also has been seen that computationally efficient engineering methods such as the mode superposition method captures the regime of chaos accurately. The availablity of such a solution scheme enables one actually to check the behavior of real life structures for chaos. Since the predictability is lost in chaotic systems, it is possible to carry out a parametric study, and to ensure that chaos is avoided in the system and predictability regained. This could be extremely useful for estimating the fatigue limited or fretting wear limited life of systems. The authors consider this to be the most important application of such studies.

REFERENCES

1. F. C. Moon and P. J. Holmes 1979 *Journal of Sound and Vibration* **65**, 275–296. A magneto-elastic strange attractor.
2. F. C. Moon 1987 *Chaotic Vibrations—an Introduction for Engineers and Applied Scientists*. New York: John Wiley.
3. D. M. Tang and E. H. Dowell 1988 *Journal of Applied Mechanics* **55**, 190–196. On the threshold force for chaotic motion for a forced buckled beam.
4. K. J. Bathe and E. L. Wilson 1978 *Numerical Methods in Finite Element Techniques*. Englewood Cliffs, NJ: Prentice-Hall.
5. R. D. Cook 1981 *Concepts and Application of Finite Element Analysis*. New York: John Wiley.
6. V. Ramamurthy 1989 *Computer Aided Design in Mechanical Engineering*. New Delhi: Tata McGraw-Hill.
7. M. Paz 1985 *Structural Dynamics*: *Theory and Computation*. New York: Van Nostrand Reinhold.
8. W. Weaver, Jr., S. P. Timoshenko and D. H. Young 1990 *Vibration Problems in Engineering*. New York: John Wiley.
9. R. I. K. Moorthy 1986 *Bhaba Atomic Research Centre Internal Report*. Early failure detection of four-loop PWRs.
10. V. Bauernfeind and R. I. K. Moorthy 1988 19*th Informal Meeting on Reactor Noise*. *Rome*, 4–6 *June*. Sensitivity studies using an analytical vibration model of a four loop PWR.
11. V. Bauernfeind 1988 *Progress in Nuclear Energy* **21**, 247–254. Vibration monitoring of four-loop PWR: model investigations of sensitivity of the monitored signals on mechanical failures.
12. T. Belytschko and W. L. Mindle 1980 *Proceedings of the ASME Winter Annual Meeting*, *ASME Publication no*. *AMD* **38**: *Damping Applications for Vibration Control*. The treatment of damping in transient computations.
13. K. J. Bathe, E. L. Wilson and F. E. Peterson 1974 *Report no*. *EERC*-73-11, *College of Engineering*, *University of California*, *Berkeley*, *LA*. SAP-IV—a structural analysis program for static and dynamic analysis of linear systems.
14. R. I. K. Moorthy, A. Kakodkar, H. R. Srirangarajan and S. Suryanarayan 1993 *Computers and Structures* **49**, 597–603. An assessment of the Newmark method for solving chaotic vibrations of impacting oscillators.
15. R. I. K. Moorthy, A. Kakodkar, H. R. Srirangarajan and S. Suryanarayan 1993 *Computers and Structures* **49**, 589–596. Finite element simulation of chaotic vibrations of a beam with non-linear boundary conditions.
16. B. J. Dobson 1984 *Proceedings of the International Conference on Numerical Methods for Transient and Coupled Problems*. *Venice*, 9–13 *July* (R. W. Lewis, E. Hinton and P. Bettess, editors). The Newmark and mode-superposition method for transient analysis analysis of a linear of linear structure—case study.
17. F. C. Moon 1985 *Applied Mechanics Review* **38**, 1284–1286. Non-linear dynamic system.